Environmental and Climate Technologies
2022, vol. 26, no. 1, pp. 708–719
https://doi.org/10.2478/rtuect-2022-0054
https://content.sciendo.com

Thermal Comfort in Indoor Spaces with Radiant Capillary Heaters

Valters DZELME[1*], Jevgenijs TELICKO[2], Andris JAKOVICS[3]

[1–3]*Institute of Numerical Modelling, University of Latvia, 3 Jelgavas street, Riga, Latvia*

***Abstract* – Capillary heat exchangers are a great alternative to conventional radiators or electric heaters when used with heat pumps due to larger area and therefore a lower working temperature. In this work, we study thermal conditions in a model room using either capillary or conventional heaters. Experimental measurements in a special test building are used to validate and adjust numerical models. The results show that the vertical temperature distribution is similar with both heating systems, but air flow velocities are considerably higher and floor temperature is less uniform in case of radiator heating. Overall, the capillary system provides more uniform thermal conditions.**

***Keywords* – Capillary heating; numerical modelling; radiator heating; thermal comfort**

Nomenclature		
ρ	Density	kg/m^3
μ	Dynamic viscosity	Pa·s
κ	Heat conductivity	W/(m·K)
α	Thermal expansivity	K^{-1}
T	Temperature	°C
v	Flow velocity	m/s
p	Pressure	Pa
g	Gravity acceleration	m/s^2
c_p	Heat capacity at constant pressure	J/(kg·K)

1. INTRODUCTION

It is always desirable to reduce energy consumption and at the same time improve thermal comfort in indoor spaces. Thermal comfort can be defined as human satisfaction with the thermal environment. It depends on different factors, such as the air temperature, humidity, air flow speed, radiant temperature and activity levels. There are different models quantifying thermal comfort, such as the Predicted Mean Vote (PMV), which predicts the thermal sensation votes from a large group of people. A related index – the Predicted Percentage of Dissatisfied (PPD), which is calculated from PMV, predicts the percentage of people dissatisfied with the thermal environment [1].

Thermal comfort in the built environment is a very active field of research. There are many field studies surveying different groups of people in different types of buildings, such as

* Corresponding author.
E-mail address: valters.dzelme@lu.lv

schools [2], [3], hospitals [4], [5], residential buildings [6], [7] and others. Many field studies find that the calculated PMV values differ from the actual mean vote. A comprehensive analysis of the accuracy of the PMV/PPD model is reported in [8]. It is found that the calculated values are accurate around 34 % of the time, although it varies between different climates and environments. This means that other factors not considered in the standard PMV/PPD model, such as radiation asymmetry and floor temperature, must be taken into account to assess thermal comfort in specific environments. Outdoor conditions can also play a role in thermal sensation indoors, which is considered by the adaptive comfort models [1].

In addition to field surveys, there are laboratory studies involving experimental measurements in controlled environments. These studies focus on quantifying thermal comfort depending on specific factors. For example, the influence of different cooling systems (convective and radiant) on thermal sensation of test subjects was studied in [9], finding that local effects, such as skin temperatures, play an important role in the overall thermal assessment. Another interesting study in a climate chamber [10] found the importance of psychological factors – the thermal sensation of the test subjects improved when they had an option to control the thermal environment, even without actually changing anything. This shows that human thermal comfort is indeed a very complicated subject, with influencing factors ranging from purely physical (air temperature, humidity etc.) to psychological.

Numerical modelling is a powerful tool for investigating physical conditions indoors. Numerical modelling is often cheaper and less time-consuming and can provide more detailed information than experiments. Thermal environment indoors has been studied numerically in many works. For example, indoor environment quality with heat recovery ventilation combined with low-temperature radiator has been analysed in [11], thermal comfort in a room heated by a conventional radiator or radiant walls/floor was studied in [12], and thermal conditions in a model room heated by air-air or water-air heat pump system, an electric heater, as well as a ceiling radiant capillary mat was investigated in [13]. Numerical models often require experimental validation, hence many studies combine experiments with modelling. Simulation data can also often complement experimental measurements. For example, simulated air velocity and radiation view factors together with temperature measurements were used in [14] to calculate PMV and assess thermal conditions in a room with radiant cooling ceiling.

Regardless of psychological and other aspects that are difficult to quantify, the physical environment (air temperature, air flow speeds, temperature gradients, radiation asymmetry, etc.) is still the most important factor determining thermal comfort, which is therefore controlled by parameters of heating, cooling and ventilation systems.

Ordinary radiators with hot water or electric heaters, that are usually located under windows or close to external walls, are very popular in northern Europe during the cold seasons. Such heaters produce a lot of air convection due to high local temperature and hot air rising. This can provide efficient air mixing and temperature homogenization but can also promote dust circulation [15], [16]. Additionally, thermal comfort can be reduced by high local temperature gradients and radiation asymmetry [13], [17] in the vicinity of the heaters.

An alternative to traditional heaters are hydronic radiant heating systems that use warm water running through pipes as the heat carrier. The pipes can be built into the constructions or attached to surfaces as panels on floors, ceilings and walls [15], [18]. There are many advantages of radiant systems. Firstly, because of larger heating area (for example, the radiant panels can cover the whole ceiling), lower water temperature is needed to heat a room compared to conventional radiators. By decreasing the water temperature, radiant systems also enable cooling in hot weather. However, additional measures, such as ventilation or

dehumidification, must be taken to prevent condensate on ceiling radiant systems in cooling mode [15].

Because the majority of heat transfer with radiant systems is through radiation, the same thermal comfort can be achieved with lower air temperature compared to traditional heating systems. Lower air temperature in a room leads to reduced heat losses through the constructions and reduced energy use [19].

The greatest benefit of hydronic radiant systems comes from using them in combination with heat pumps. It is well known that the efficiency of a heat pump decreases with increasing the temperature difference it has to maintain [20]. Since radiant heating systems require lower working temperature than conventional heaters, heat pumps can operate more efficiently. This can be a cheaper alternative to heating by non-renewable resources, such as natural gas.

Reduced convection with ceiling radiant heaters can lead to vertical temperature gradients or stratification, which may induce thermal discomfort [21]. This can be controlled by optimizing the size and location of the panels [22] or with ventilation.

A more recent development are radiant capillary heat exchangers, which consist of networks of thin tubes, sometimes called capillary micro tubes [23] (typical diameter 3–5 mm), made of polypropylene or polyethylene that can be installed as panels or mats on ceilings, walls and floors [24]. The advantages of capillary over the pipe systems are even lower water temperature (up to 35 °C [25]) and the flexibility of installation on various surfaces.

Many studies involving capillary systems consider floor heating. Capillary system (a network of tubes with diameter 3.6 mm, 20 mm apart) was compared with regular radiant system (pipes with diameter 16 mm, 200 mm apart) for floor heating in a numerical and experimental study reported in [26]. Capillary system showed nearly uniform temperature distribution and its responsiveness (time it takes to heat the room), as well as provided thermal comfort was superior to the regular radiant system. Similar findings are reported in [27].

Floor radiant heating was compared with ceiling and wall capillary system in [28], finding that capillary system provides heating demands at a reduced energy consumption, however, causing stronger vertical temperature stratification than the floor system.

Unlike for cooling, literature on ceiling capillary systems for heating is rather scarce. Some studies, such as [29], study ceiling capillary heating experimentally, finding that it provides good thermal comfort according to standards. Considering the energy advantages of capillary heating, the subject requires more research, especially long-term experiments in colder climates and thorough numerical investigations.

In this work, we investigate thermal conditions in a model room heated with either capillary system on the ceiling and one wall or an ordinary radiator below a window. The model room is a test building in Riga, Latvia and we consider a period in winter. We build 3D numerical models and compare the results with measurements from the experimental building where both heating systems along with different sensors are installed. We analyse temperature and air flow distribution, heating power and other factors to assess the benefits and disadvantages of each heating system. In long-term experimental studies, numerical models will be used to optimize the parameters of the capillary system.

2. EXPERIMENTAL BUILDING

On the grounds of the Botanical Garden of the University of Latvia in Riga there are five single-room test buildings each built with different materials, such as aerated concrete and plywood panels. A picture of one of the buildings from outside is shown on the left in Fig. 1. Detailed information about the buildings and the materials used can be found in [30]. In this

work, we will use the building with plywood frame as the model room, because it has capillary mats installed on the ceiling and one wall. The capillaries are connected to air-water heat pump which is used as the heat source.

The model room has a door, a window, ventilation inlet and outlet, as well as a conventional heater below the window and capillary mats on the ceiling and one wall. Scheme of the room is shown on the right in Fig. 1.

The capillary mats consist of polypropylene tubes with diameter of 3 mm placed 20 mm apart. There are three connected mats – two on the ceiling and one on the wall close to the window. The water running through the capillaries is heated by a heat exchanger connected to an air-water heat pump. At this stage, the mats are not built into any material, i.e. they are exposed to the air.

Throughout the test building there are temperature, humidity, pressure and air flow speed sensors. A web-based monitoring system to gather sensor data was set up in 2013 [31]. Temperature is measured by SHT75 digital sensors with measurement accuracy of ±0.3 °C. Sensors used in this work are fixed in the middle of the room at different heights from the floor: 0.1 m, 0.6 m, 1.1 m, 1.7 m, 2.9 m.

(a) (b)

Fig. 1. A test building from a) outside and b) a scheme of the inside.

An independent monitoring system with ultrasonic heating/cooling meter *LandisGyr T550* with accuracy class 2 (EN 1434) and measurement error below 6 % is used for collecting energy consumption data of the capillary system. Temperature and heating energy was measured every 1 minute and the measurements were synchronised using a network time protocol (NTP) server. Data from each sensor is stored in a central FTP server.

A thermal camera *FLIR T650sc* with measurement error of ±0.2 °C was used to capture temperature of various surfaces inside the model room, including the temperature distribution of the capillary mats.

The heat transfer coefficients used in the boundary conditions of the numerical model were measured experimentally as reported in [32].

3. NUMERICAL MODEL

The scheme of the numerical domain is shown on the right in Fig. 1. Many small items, such as electronic boxes, are also present in the room but are not included in the numerical model for simplicity. To take into account the heat generated in those items, it can be added as a heat source.

The relevant physical processes in the room are turbulent fluid flow and heat transfer with radiation. From many options, we have selected *ANSYS CFX* as the main tool to simulate these processes. Since we want to study a case of thermal equilibrium, the simulations will be steady.

There are two possible mechanisms of air convection in this system: natural convection (thermal buoyancy) and forced convection (ventilation). In this work, we will not consider ventilation. Natural convection is driven by gravity acting on the fluid with temperature-dependent density. In a compressible case, density is calculated from equations of state. Due to low speeds (compared to the speed of sound) and small density variations (air density changes only a few percent from 10 °C to 25 °C), in our case we can consider the air to be incompressible and use the Boussinesq approximation, which assumes constant density everywhere in the equations except in the buoyancy force term.

The steady incompressible fluid flow is then described by the Navier-Stokes equations

$$(\vec{v}\cdot\nabla)\vec{v} = -\frac{1}{\rho}\nabla p + \mu\Delta\vec{v} + \overrightarrow{f_g}\,, \tag{1}$$

$$\nabla\cdot\vec{v} = 0\,, \tag{2}$$

where

$\overrightarrow{f_g} = \left(1-\alpha\left(T-T_{\text{ref}}\right)\right)\vec{g}$ buoyancy force term;

T_{ref} reference temperature.

To obtain temperature T, CFX solves the energy equation for enthalpy h. Neglecting viscous dissipation, compressibility effects and assuming constant material properties, as well as the relation between enthalpy and temperature $h = c_{\text{p}}(T - T_{\text{ref}})$, the steady energy equation can be written for temperature

$$(\vec{v}\cdot\nabla)T = \frac{k}{\rho c_{\text{p}}}\nabla T + S\,, \tag{3}$$

where S volumetric heat sources.

To include thermal radiation, we use the Discrete Transfer model in CFX, which solves a radiative transport equation containing terms for absorption, emission and scattering. Since air is optically very thin, the simulation time can be improved by considering air to be completely transparent and not participating in radiative processes directly. In such a case, at the start of the simulation, a number of radiation ray paths from all surfaces are generated. These paths connect points between all surfaces. During the simulation, these paths are used to calculate radiative energy emitted and absorbed by each surface element depending on their relative temperatures. Number of rays from each boundary element is set to 50.

With typical Reynolds numbers on the order of 10^5, the air flow is turbulent. For most practical applications, Reynolds Averaged Navier-Stokes (RANS) eddy-viscosity models are

precise enough. Among different RANS models, we select the k-ω SST model, as it is considered to be the best with wall bounded flows with heat transfer [33].

The best accuracy can be achieved by using a mesh with the dimensionless first cell distance from the wall $y^+ < 1$, which means that boundary layers layers are fully resolved without using wall functions. However, it can be difficult to achieve convergence with such a mesh. We have found that a coarser mesh with wall function approach gives results that differ only about 2 % compared to the fully resolved case, and simulation time is considerably smaller. The mesh used in this work contains 184 thousand elements with characteristic element size of 5 cm and two elements of 1.5 cm normal to the boundaries.

Reference temperature for the Boussinesq approximation is $T_{ref} = 20$ °C. Velocity boundary condition is no-slip on all surfaces, including the inlet and outlet (ventilation is not considered in this work). Temperature boundary conditions are following. On floor, ceiling and walls: convection boundary condition with reference temperature T_{out}, heat transfer coefficient $U = 0.15$ W/(m^{2}K) and emissivity $\varepsilon = 0.9$. On window and door: convection condition with reference temperature T_{out}, $U = 0.8$ W/(m^{2}K) and emissivity $\varepsilon = 0.9$.

We consider both capillary and conventional heating. The capillary panels are modelled as uniform surfaces, without resolving the capillary tubes. When capillary heating is active, boundary condition on the panels are constant temperature T_{cap} and emissivity $\varepsilon = 0.9$, and insulation condition on the conventional heater. With conventional radiator heating, capillary panels have the same conditions as walls and a constant temperature $T_{rad} = 41.8$ °C is set on the radiator surface, which results in the same average room temperature as with capillary heating.

4. RESULTS

4.1. Experimental Results

The capillary heat exchanger mats contain small tubes with running water. At this stage, the capillaries are not built into any material and are simply attached to the surfaces. Ideally, we would like the panels to have uniform temperature distribution. In reality, the temperature of the tubes is higher than in the space between them, as well as the returning water is cooler. We have captured thermal images of the panels and other places in the room. Fig. 2 shows normal and thermal images of some sections of the ceiling capillaries.

From the thermal images, we can extract the average temperature of the panels. The overall average temperature in the rectangular areas selected in the thermal images on the right of Fig. 2 is 23.5 °C. This value will be used in the numerical model as T_{cap}.

Thermal images were also acquired for many other surfaces and objects in the room. Fig. 3 shows thermal images of the corner furthest from the window. The most notable features here are the heat sinks in the corners. The average temperature in the selected circles in the thermal images is 19.8 °C, which can roughly be assumed to be the average room temperature.

Long term monitoring data are available from the test building. To compare the measurements to the steady-state simulations, we must select stable data from some time period when there was no direct sunlight through the window, no people in the room etc.

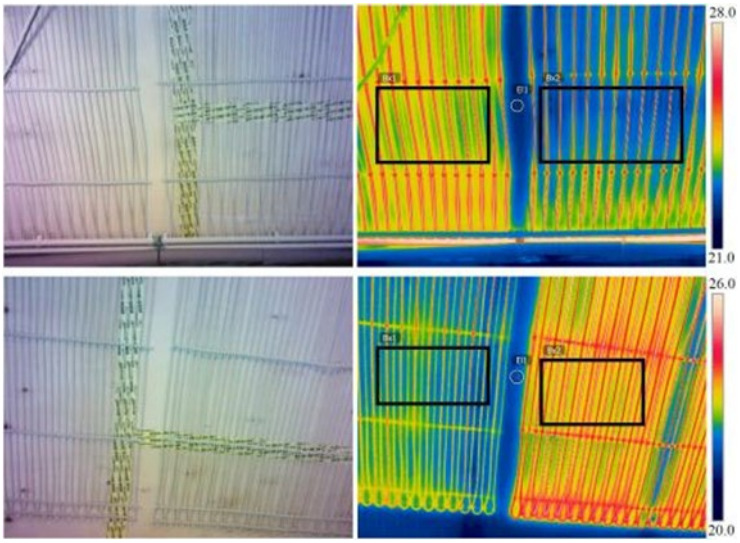

(a) (b)

Fig. 2. a) Normal and b) thermal images of the ceiling capillary tubes.

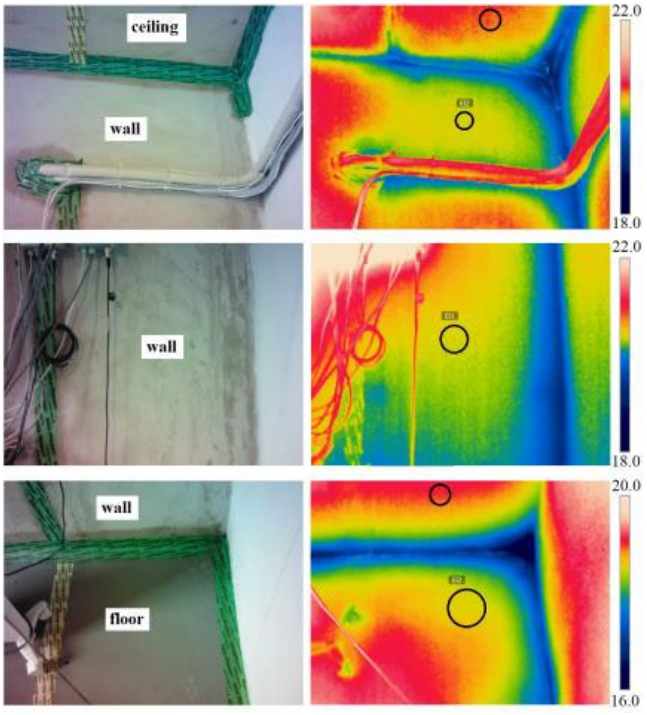

(a) (b)

Fig. 3. a) Normal and b) thermal images of the corner furthest from the window.

Fig. 4 shows temperature at different heights in the middle of the room and outside during a three day period in January 2022 with capillary heating. We have selected a 24 h period

when temperature in the room is reasonably stable. Short period oscillations, such as the four peaks within the selected 24 h period, are due to the heat pump adjustments. Longer period temperature changes, such as the rising after the 24 h period, are due to changes in the weather outside. The temperatures averaged over the selected 24 h period are plotted in Fig. 5. The average outside temperature of −0.9 °C and is used as the reference temperature T_{out} in boundary conditions of the numerical model.

The average humidity in the whole room during the 24 h period was around 23 %. Such a low value is due to absence of people and other humidity sources in the room.

Another important variable is the heat flux from the heating system. This can be calculated from the measurements of energy consumption of the capillary system. In 19 h during the selected 24 h period, the system consumed approximately 3 kWh, which corresponds to an average power of around 157 W. This includes not only the capillary mats, but also the pipes leading to them. Additional heating from electronics etc. is estimated at around 30 W, which will be included in simulations as an additional heat source spread throughout the room.

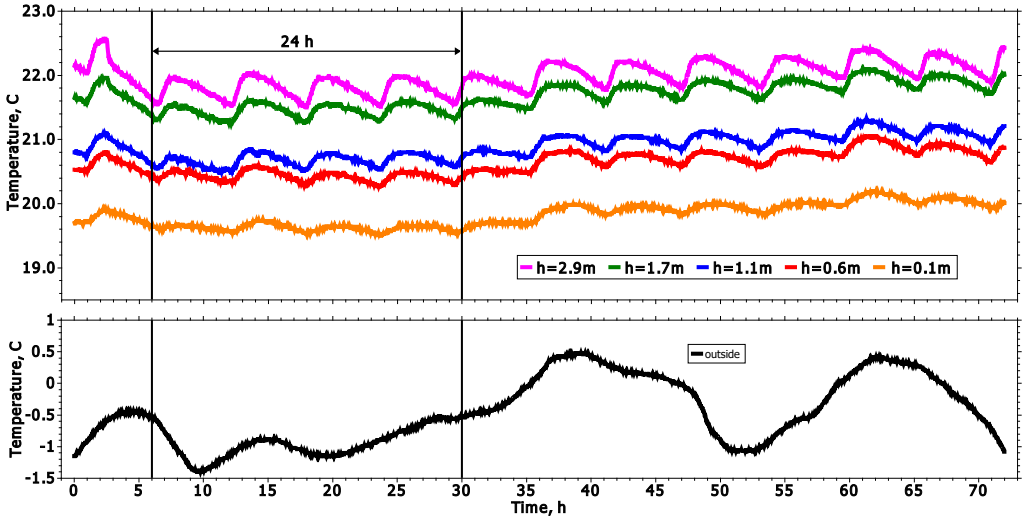

Fig. 4. Temperature outside and at different heights in the middle of the room in January 8–10, 2022.

4.2. Numerical Results

A lot more data can be obtained numerically than experimentally. Distributions of temperature or any other relevant variable can be extracted from numerical results. However, numerical models usually require some validation to ensure that the results are reliable. For this we want to select some data from experiments which can be directly compared to simulations, such as temperature measurements along the height of the room. Integral heating power of the capillary system is 140 W in simulations, which is close to the experimental value of 157 W.

In addition to capillary heating, simulations were also done for the case ordinary radiator or electric heater with the capillary system off.

Fig. 5 shows vertical temperature distribution in the middle of the room. Qualitatively, the simulated vertical distribution of temperature is in agreement with the measurements for the capillary heating case. Quantitatively, overall, the agreement can also be considered good. Near the floor and the ceiling, the agreement is very good, but in the middle of the room the

measured values are higher, but only by less than a degree. A closer agreement may not be possible due to simplifications in the model, such as no solar radiation through the window, no moisture in the air and walls, as well as geometrical simplifications and the approximation of additional heat sources as a non-localised integral value. Including various geometrical features in the model would make it more difficult to generate good quality mesh, which was found to be crucial to achieve convergence.

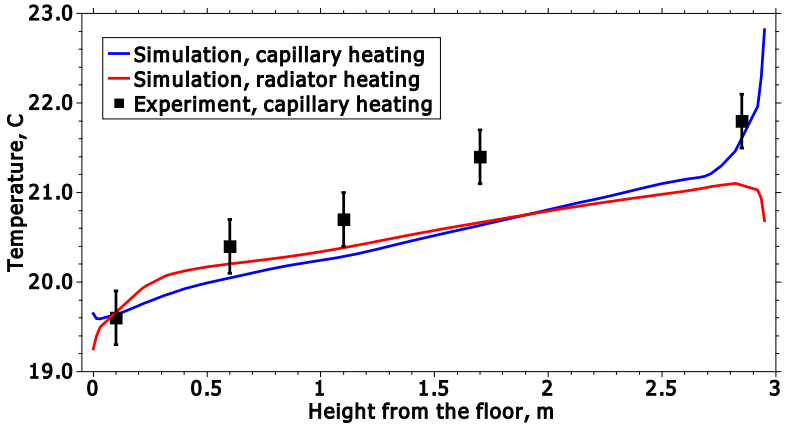

Fig. 5. Vertical temperature distribution in the middle of the room.

The vertical temperature gradient in the middle of the room with capillary heating is 0.57 °C/m, considering heights from 10 cm to 2.7 m. In experiments it is 0.78 °C/m. However, the measurement error is 0.3 degrees and there must also be some uncertainty in the sensor positions in the room. The difference can also be explained by the assumption of uniform temperature of the capillary mats in simulations. Local temperature variations in the real pipe system can lead to slightly different temperature distribution. With radiator heating, the vertical gradient in the middle of the room is 0.44 °C/m. The vertical temperature difference between head (1.7 m) and ankles (10 cm) is therefore below the maximum allowable 3 °C according to [1] for local thermal comfort with both heating systems. However, temperature distribution is considerably different near the radiator.

Fig. 6 shows temperature distribution on two vertical planes and the floor with both heating systems. Note that the value range is different in each image. The vertical temperature gradient is almost the same in most of the room, except near the window in case of radiator heating.

Standards [1] require floor temperature to be between 19 °C and 29 °C. The average floor temperature is 19.6 °C with capillary mats and 19.4 °C with radiator, both of which are within the recommended limits. However, the temperature variations on the floor are wider with radiator heating, with the ranges shown in Fig. 6. The condition $T \geq 19$ °C is satisfied on 97 % of the floor with capillary mats and only 50 % of the floor with radiator. Clearly, the capillary heating system provides more uniform temperature distribution.

Location of the radiator near the wall below the window not only leaves large area of the floor near the door cooler, but also the wall behind the radiator can be overheated, leading to unnecessary heat losses. With lower temperature capillary system, this effect is not as strong.

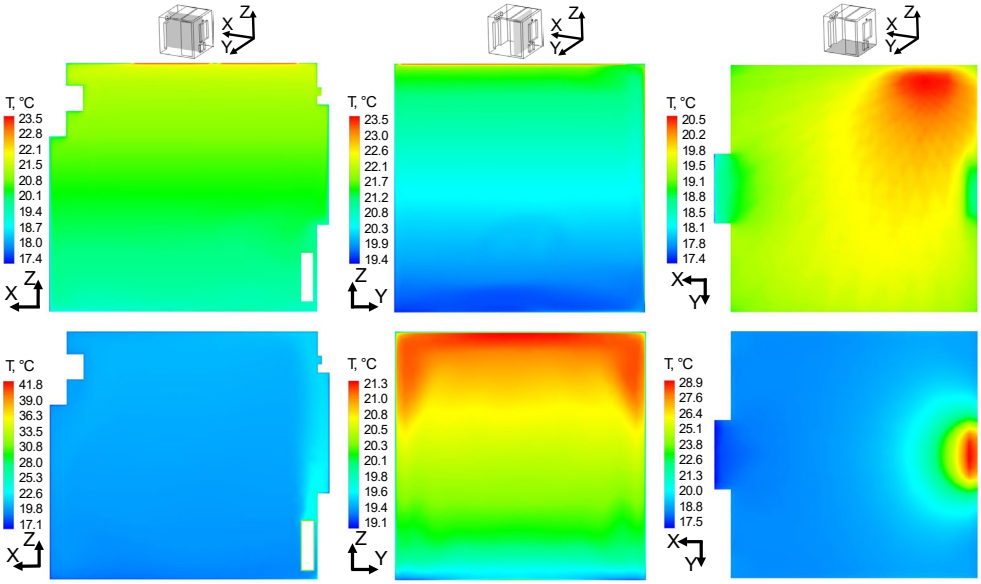

Fig. 6. Temperature distribution in the room: with capillary mats (top row) and radiator heating (bottom row). Note that the value range is different in each image.

Simulated average temperature in the room is 20.5 °C with both heating systems. The average temperature in experiments is 19.8 °C, which was estimated from the thermal images of walls, ceiling and floor. A lower value in experiments could be due the heat sinks in the corners which are not present in the model.

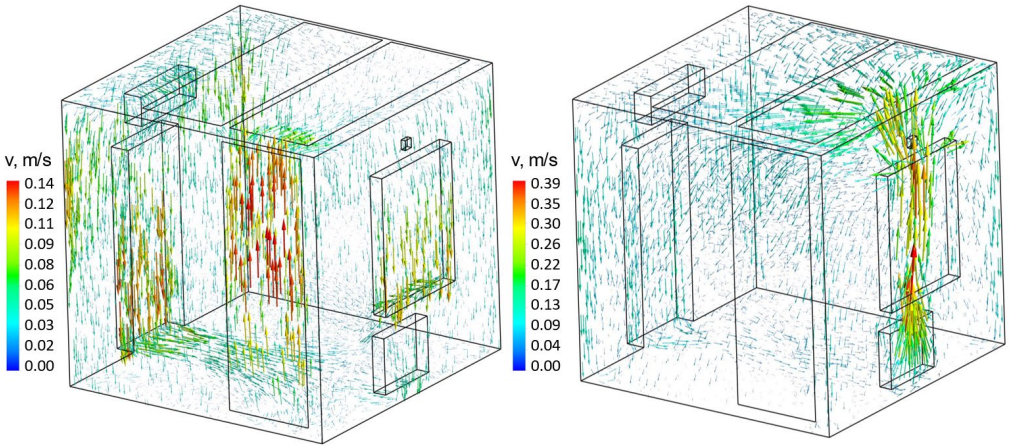

Fig. 7. Velocity distribution in the room: a) with capillary mats and b) radiator heating.

Air flow velocity is another important factor affecting comfort. Velocity vectors in the room are shown in Fig. 7. In case of capillary heating, notable upwards flow is present near the wall capillary panel and downwards flows by the door and window. In case of radiator

heating, the air flow is dominated by the rising air above the heater with maximum velocity of 39 cm/s, which is almost three times of the capillary case. It is this strong upwards convection above the radiator that causes vertical temperature stratification as shown in bottom center of Fig. 6. In case of capillary mats, the stratification is mostly due to heated ceiling.

5. CONCLUSIONS

In this work, thermal conditions in a model room heated by either capillary mats on the ceiling, and one wall or conventional heater below the window have been studied. Experimental data from a test building with capillary mats was compared to 3D simulations. The results agree reasonably well regarding the vertical temperature distribution and total heating power.

The main numerical result is that, compared to conventional heating, capillary mats produce less air convection with similar vertical temperature gradient in the middle of the room. With radiator heating, the floor temperature between 19 °C and 29 °C, as required by standards, is satisfied only on 50 % of the floor. This can lead to reduced local comfort conditions. Capillary heating in this case produces more uniform thermal environment. However, more thorough parametric studies are necessary to collect more data and draw more concrete conclusions about the applicability and thermal comfort with capillary mats.

Further work will include long-term monitoring of thermal environment in the experimental buildings with capillary heating, as well as cooling in warm weather. Various parameters, such as the water temperature and location of the mats, will be optimized using numerical models. The main goal of this research is to understand how feasible it is to use capillary heating in Latvian climate compared to traditional heating with radiators.

ACKNOWLEDGEMENT

This work has been financially supported by the ERDF project “Development of methodology for calculating the heating/cooling capacity of the capillary water heat exchanger, taking into account the building, climate and performance characteristics” No. 1.1.1.1/19/A/102.

REFERENCES

[1] ASHRAE Standard 55-2010. Thermal environmental conditions for human occupancy. American Society of Heating, Refrigerating and Air-Conditioning Engineers, 2010.

[2] Katafygiotou M. C., Serghides D. K. Thermal comfort of a typical secondary school building in Cyprus. *Sustainable Cities and Society* 2014:13:303–312. https://doi.org/10.1016/j.scs.2014.03.004

[3] Vilcekova S., *et al.* Indoor environmental quality of classrooms and occupants' comfort in a special education school in Slovak Republic. *Building and Environment* 2017:120:29–40. https://doi.org/10.1016/j.buildenv.2017.05.001

[4] Del Ferraro S., *et al.* A field study on thermal comfort in an Italian hospital considering differences in gender and age. *Applied Ergonomics* 2015:50:177–184. https://doi.org/10.1016/j.apergo.2015.03.014

[5] Zaniboni L., *et al.* Subjective and objective assessment of thermal comfort in physiotherapy centers. *Building and Environment* 2020:176:106808. https://doi.org/10.1016/j.buildenv.2020.106808

[6] Zhang Y., *et al.* Thermal comfort in naturally ventilated buildings in hot-humid area of China. *Building and Environment* 2010:45(11):2562–2570. https://doi.org/10.1016/j.buildenv.2010.05.024

[7] Li B.,, *et al.* Indoor thermal environments in Chinese residential buildings responding to the diversity of climates. *Applied Thermal Engineering* 2018:129:693–708. https://doi.org/10.1016/j.applthermaleng.2017.10.072

[8] Cheung T., *et al.* Analysis of the accuracy on PMV – PPD model using the ASHRAE Global Thermal Comfort Database II. *Building and Environment* 2019:153:205–217. https://doi.org/10.1016/j.buildenv.2019.01.055

[9] Schellen L., *et al.* The influence of different cooling techniques and gender on thermal perception. *Building Research & Information* 2013:41(3):330–341. https://doi.org/10.1080/09613218.2013.772002

[10] Zhou X., *et al.* Experimental study of the influence of anticipated control on human thermal sensation and thermal comfort. *Indoor Air* 2014:24(2):171–177. https://doi.org/10.1111/ina.12067
[11] Jahanbin A., Semprini G. Numerical study on indoor environmental quality in a room equipped with a combined HRV and radiator system. *Sustainability* 2020:12(24):10576. https://doi.org/10.3390/su122410576
[12] Sobhi M., Khalil E. E. Air flow patterns and thermal comfort in a room with diverse heating systems. *AIAA Scitech Forum* 2020. https://doi.org/10.2514/6.2020-1221
[13] Sabanskis A., Virbulis J. Experimental and numerical analysis of air flow, heat transfer and thermal comfort in buildings with different heating systems. *Latvian Journal of Physics and Technical Sciences* 2016:2:20–30. https://doi.org/10.1515/lpts-2016-0010
[14] Catalina T., Virgone J., Kuznik F. Evaluation of thermal comfort using combined CFD and experimentation study in a test room equipped with a cooling ceiling. *Building and Environment* 2009:44(8):1740–1750. https://doi.org/10.1016/j.buildenv.2008.11.015
[15] Rhee K.-N., Olesen B. W., Kim K. W. Ten questions about radiant heating and cooling systems. *Building and Environment* 2017:112:367–381. http://dx.doi.org/10.1016/j.buildenv.2016.11.030
[16] Nou T., Viljasoo V. The effect of heating systems on dust, an indoor climate factor. *Agronomy Research* 2011:9:165–174.
[17] Wang Y., *et al.* Numerical simulation of thermal performance of indoor airflow in heating room. *Energy Procedia* 2019:158:3277–3283. https://doi.org/10.1016/j.egypro.2019.01.983
[18] Oxizidis S., Papadopoulos A. M. Performance of radiant cooling surfaces with respect to energy consumption and thermal comfort. *Energy and Buildings* 2013:57:199–209. https://doi.org/10.1016/j.enbuild.2012.10.047
[19] Joe J., Karava P. A model predictive control strategy to optimize the performance of radiant floor heating and cooling systems in office buildings. *Applied Energy* 2019:245:65–77. https://doi.org/10.1016/j.apenergy.2019.03.209
[20] Zhao M., *et al.* Performance comparison of capillary mat radiant and floor radiant heating systems assisted by an air source heat pump in a residential building. *Indoor and Built Environment* 2017:26:1292–1304. https://doi.org/10.1177/1420326X16674517
[21] Gendelis S., *et al.* Monitoring results and analysis of thermal comfort conditions in experimental buildings for different heating systems and ventilation regimes during heating and cooling seasons. *IOP Conf. Series: Materials Science and Engineering* 2017:251:012053. https://doi.org/10.1088/1757-899X/251/1/012053
[22] Tye-Gingras M., Gosselin L. Comfort and energy consumption of hydronic heating radiant ceilings and walls based on CFD analysis. *Building and Environment* 2012:54:1–13. https://doi.org/10.1016/j.buildenv.2012.01.019
[23] Mikeska T., Svendsen S. Study of thermal performance of capillary micro tubes integrated into the building sandwich element made of high performance concrete. *Applied Thermal Engineering* 2013:52(2):576–584. https://doi.org/10.1016/j.applthermaleng.2012.12.029
[24] Li N., Chen Q. Study on dynamic thermal performance and optimization of hybrid systems with capillary mat cooling and displacement ventilation. *International Journal of Refrigeration* 2020:110:196–207. https://doi.org/10.1016/j.ijrefrig.2019.10.016
[25] Zhao M., *et al.* Experimental investigation and feasibility analysis on a capillary radiant heating system based on solar and air source heat pump dual heat source. *Applied Energy* 2017:185:2094–2105. https://doi.org/10.1016/j.apenergy.2016.02.043
[26] Cho J., Park B., Lim T. Experimental and numerical study on the application of low-temperature radiant floor heating system with capillary tube: Thermal performance analysis. *Applied Thermal Engineering* 2019:163:114360. https://doi.org/10.1016/j.applthermaleng.2019.114360
[27] Zhou G., He J. Thermal performance of a radiant floor heating system with different heat storage materials and heating pipes. *Applied Energy* 2015:138:648–660. https://doi.org/10.1016/j.apenergy.2014.10.058
[28] Zhao M., *et al.* Performance comparison of capillary mat radiant and floor radiant heating systems assisted by an air source heat pump in a residential building. *Indoor and Built Environment* 2017:26:1292–1304. https://doi.org/10.1177%2F1420326X16674517
[29] Weibin K., *et al.* Experimental investigation on a ceiling capillary radiant heating system. *Energy Procedia* 2015:75:1380–1386. https://doi.org/10.1016/j.egypro.2015.07.220
[30] Jakovičs A., *et al.* Monitoring and Modelling of Energy Efficiency for Low Energy Testing Houses in Latvian Climate Conditions. *International Journal of Energy* 2014:8:76–83.
[31] Greitans M., *et al.* Web-based real-time data acquisition system as tool for energy efficiency monitoring. *21st telecommunications forum TELFOR* 2013. https://doi.org/10.1109/TELFOR.2013.6716289
[32] Gendelis,S., Jakovičs A., Ratnieks J. Results of long-term energy efficiency monitoring of test buildings under real climatic conditions. *International Multidisciplinary Scientific GeoConference Surveying Geology and Mining Ecology Management*, *SGEM* 2017:17:643–650. https://doi.org/10.5593/sgem2017H/63/S26.081
[33] Menter F. R., Matyushenko A. ANSYS CFX Documentation, Version 18.0, Section 4 “Turbulence and Near-Wall Modeling”. Ansys, 2022.